Chinese Chemical Letters 37 (2026) 111499

Contents lists available at ScienceDirect

Chinese Chemical Letters

journal homepage: www.elsevier.com/locate/cclet

[7]Cyclophenoxathiin: A heptagonal frustum-shaped nanobelt container for fullerenes

Zhenglin Du[a], Weijie Zhang[a], Yisong Tang[a], Xia Li[a], Jialin Xie[b,*], Kelong Zhu[a,*]

[a] School of Chemistry, Sun Yat-sen University, Guangzhou 510275, China
[b] Hainan Provincial Key Laboratory of Fine Chem, School of Chemistry and Chemical Engineering, Hainan University, Haikou 570228, China

ARTICLE INFO

Article history:
Received 8 March 2025
Revised 9 June 2025
Accepted 23 June 2025
Available online 24 June 2025

Keywords:
Nanobelt
Phenoxathiin
Host-guest complex
Fullerene
Heterocycle

ABSTRACT

Nanobelts have attracted significant attention in both synthetic and supramolecular chemistry due to their distinctive structures and promising applications. However, their synthesis remains challenging due to the high strain inherent in their ribbon-like configurations. A promising approach to mitigate this strain involves incorporating heteroatoms, such as sulfur and oxygen, which not only alleviate strain but also introduce new functionalities. In this study, we report the synthesis of a novel C_2-symmetric nanobelt, [7]cyclophenoxathiin (**[7]CP**), through a multi-step process. The structure of **[7]CP** was confirmed using NMR, mass spectrometry, and single-crystal X-ray diffraction, revealing a heptagonal frustum-shaped geometry. Host-guest interactions between **[7]CP** and selected fullerenes were investigated using UV–vis absorption, ^{1}H NMR, and X-ray crystallography. Our findings demonstrate that **[7]CP** forms 1:1 complexes with fullerenes, exhibiting moderate binding through $\pi-\pi$ interactions, with binding constants of 1638, 2534, and 3682 L/mol for C_{60}, C_{70}, and $PC_{61}BM$, respectively. The reduced cavity size of **[7]CP** prevents the formation of dimeric complexes observed with [7]cyclophenoxathiin, while still allowing it to function effectively as a molecular container.

© 2026 Published by Elsevier B.V. on behalf of Chinese Chemical Society and Institute of Materia Medica, Chinese Academy of Medical Sciences.

Nanobelts, such as cyclacenes [1–8] and beltarenes [9], along with their partially or fully hydrogenated analogs [10–14], have emerged as prominent subjects in both synthetic and supramolecular chemistry due to their intriguing molecular structure and promising applications in supramolecular containers, nanomaterials, and organic semiconductors [15]. More importantly, nanobelts can also serve as template molecules for the bottom-up construction of nanotubes [16,17]. Despite the growing interest in this field, the development of nanobelts has been slow, primarily due to synthetic challenges. Specifically, inducing high tension in these ribbon-like structures can often leads to low synthetic yields, which significantly hinder further derivatization and broader application. Therefore, the development of nanobelts with diverse structures remains a significant challenge.

To address the strain issues associated with the synthesis of nanobelts, carbon atoms could be partially replaced by heteroatoms to create a hybrid belt structure. In addition to relieving ring strain through geometric adjustments, the incorporation of heteroatoms introduces new functionalities, ultimately yielding multifunctional macrocyclic materials with enhanced properties. Benefiting from such a structural design, significant progress has been made in the construction of those highly strained nanobelts [18–21]. For example, three *N*-doped nanobelts have been successfully prepared by Miao [22], Chen [23], and Wu *et al.* [24], respectively. Tanaka *et al.* demonstrated the successful construction of oxygen-embedded nanobelts by intra-molecular alkyne cyclotrimerization [25]. Subsequently, oxygen-doped belt[8]arene and belt[12]arene were reported by Wang [26] and Tiefenbacher *et al.* [27], respectively. More recently, sulfur-doped zigzag nanobelts consisted of phenoxathiin, a foldable building block bridged by oxygen and sulfur that favors a bent configuration, were also successfully accomplished (Fig. 1) [28]. The fusion of eight phenoxathiin units results in an octagonal bowl-shaped nanobelt, [8]cyclophenoxathiin (**[8]CP**), which serves as an excellent molecular container for fullerene guests [28,29]. Following this, two **[8]CP** analogues, incorporating naphthalene [30] or thianthrene [31] moieties, were successfully synthesized, further demonstrating the advantages of applying the foldable subunit in the construction of zigzag nanobelts. Despite the progress with **[8]CP**, the synthesis of [*n*]cyclophenoxathiins (**[*n*]CP**) with a number of repeating oxathiin units (*n*) greater or smaller than eight has not met success yet. Moreover, theoretical calculations demonstrate that syn-

* Corresponding authors.
E-mail addresses: xiejialin@hainanu.edu.cn (J. Xie), zhukelong@mail.sysu.edu.cn (K. Zhu).

https://doi.org/10.1016/j.cclet.2025.111499
1001-8417/© 2026 Published by Elsevier B.V. on behalf of Chinese Chemical Society and Institute of Materia Medica, Chinese Academy of Medical Sciences.

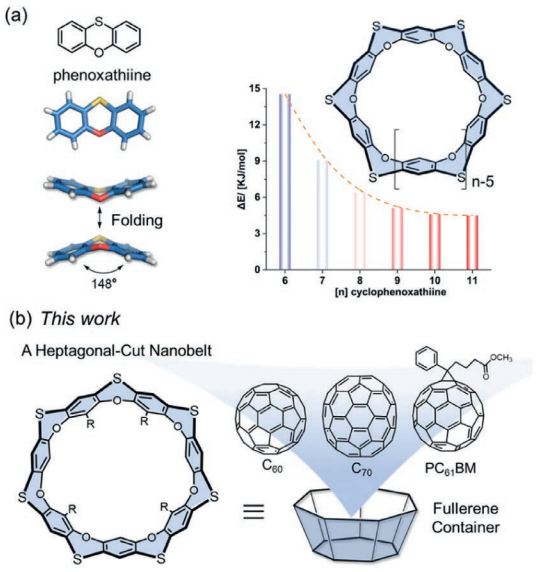
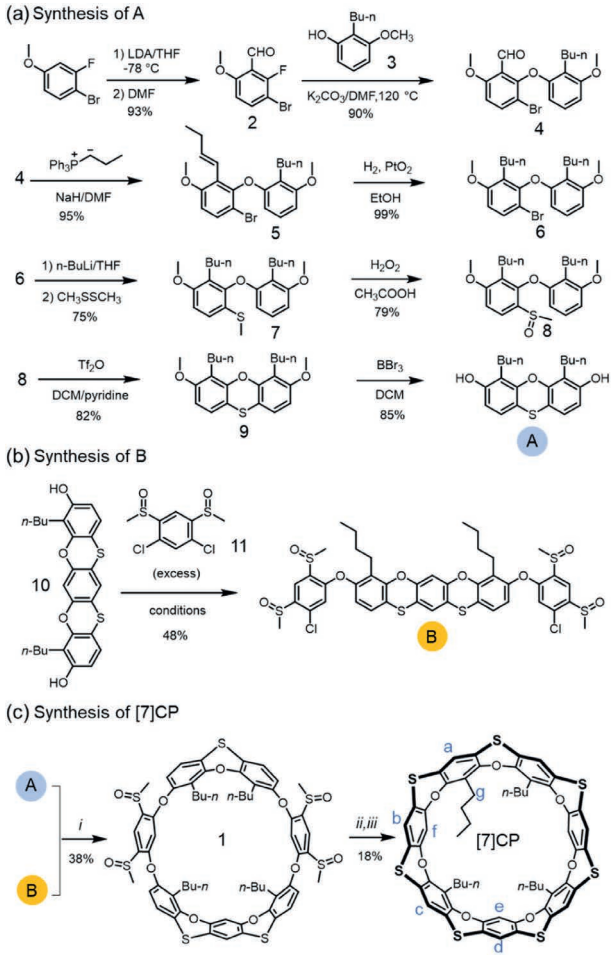


Fig. 1. (a) Structure of phenoxathiin and the ring strain diagram of [*n*]cyclophenoxathiin ($n = 6 \sim 11$); (b) the [7]cyclophenoxathiin (**[7]CP**) and its host-guest chemistry towards fullerenes reported in this work.

thesizing smaller belts is more challenging than constructing larger ones (Fig. 1 and Table S2 in Supporting information) [32]. In addtion, the synthesis of cyclophenoxathiins with odd numbers of repeating units poses an even greater challenge, as it usually requires a more tedious synthetic approach to yield the double-stranded nanobelts [33]. Therefore, we report here the synthesis of a novel C_2-symmectric [7]cyclophenoxathiin (**[7]CP**) and its host-guest chemistry towards three fullerenes.

As outlined in Scheme 1, to obtain the C_2-symmetric belt skeleton composed of seven laterally fused phenoxathiin units, a multi-step synthesis was employed, involving the preparation of two key building blocks, **A** and **B**. Initialed from the 4–bromo-3-fluoro-methoxybenenze, the diphenolic **A** can be obtained in 8 steps with a conbinded yield of 29%. **A** features a phenoxathiin skeleton with two substituted *n*–butyl groups, which serve not only to block the reaction sites between the methoxy and aryloxy groups but also to ensure the solubility of the final product. Treatment of the previously reported intermediate **10** [28] with an excess amount of **11** affords the second building block **B** in a moderate yield of 48%. Finally, a cyclization-followed-by-bridging approach was employed to construct **[7]CP**. The '1+1′ cyclization between **A** and **B**, *via* the Ullmann coupling reaction, generates the oxo-bridged macrocyclic intermediate **1**, which serves as the precursor to **[7]CP** in a 38% yield. The subsequent intramolecular Friedel-Crafts reaction on intermediate **1** completes the bridging step, yielding **[7]CP** with an isolated yield of 18%. The correct structure of **[7]CP** was confirmed through NMR, mass spectrometry, and single crystal X-ray diffraction analysis.

The ^{1}H NMR spectrum of **[7]CP** exhibits six singlets in the aromatic region with an integration ratio of 2:1:2:2:2:1, confirming a C_2-symmetric structure (Fig. 2a). The resonance peaks at 7.11, 7.08, 6.95, and 6.94 ppm were assigned to the upper-rim protons H_b, H_d, H_a, and H_c, respectively, while the signals at 6.90 and 6.87 ppm corresponded to the lower-rim protons H_f and H_e (Fig. S30 in Supporting information). MALDI-TOF-MS analysis showes a prominent peak at *m*/*z* of 1078.1284, further confirming the expected structure of **[7]CP** (Fig. 2b). Suitable single crystals of **[7]CP** were obtained through vapor diffusion of ethanol into a nitrobenzene solution of **[7]CP**. X-ray crystallography analysis revealed that **[7]CP** adopts a hepta-cut bowl-shaped geometry, with a cavity diameter of 11.7 Å measured from the upper rim (Fig. 3). This represents a decrease of 1.4 Å from the 13.1 Å cavity diameter observed for **[8]CP** [28]. The bending angles of the phenoxathiin units are approximately 130°, reduced by 7°, indicating a strained ring structure for **[7]CP** compared to that of **[8]CP**, consistent with theoretical studies (Fig. 1 and Table S2). Interestingly, the crystal packing structure of **[7]CP** shows a head-to-head dimeric capsule-like assembly, stabilized by C–H···S hydrogen bonds between the upper rims. Two nitrobenzenes are encapsulated in the cavity of the supramolecular capsule, forming a 2:2 complex, which highlights the potential of **[7]CP** as a molecular container.



Scheme 1. Synthesis of building blocks **A** and **B** and the nanobelt **[7]CP**. Conditions: (i) Cs_2CO_3, DMAC, 150 °C for 48 h; (ii) CF_3SO_3H, 80 °C for 60 h; (iii) pyridine/H_2O, 105 °C for 15 h.

Previously, we explored the host-guest chemistry between **[8]CP** and fullerenes. Due to their excellent size complementarity, two **[8]CP** units can bind one fullerene molecule, such as C_{60} or C_{70}, to form a ternary complex with strong affinity through $\pi-\pi$ and CH$-\pi$ interactions (Fig. 4a) [28,29]. Building on this, it is straightforward to investigate the binding capabilities of the relatively smaller **[7]CP** towards fullerene guests. To this end, the host-guest interactions between **[7]CP** and three selected fullerenes (C_{60}, C_{70}, and $PC_{61}BM$) were evaluated using UV–vis absorption, ^{1}H NMR, and X-ray crystallography analyses.

The UV–vis absorption analysis revealed a binding stoichiometry of 1:1 for all complexes formed between **[7]CP** and C_{60}, C_{70}, or $PC_{61}BM$ (Figs. S1, S3 and S5 in Supporting information). Subsequently, ^{1}H NMR analysis of the equimolar mixture of **[7]CP** with C_{60}, C_{70}, or $PC_{61}BM$ was performed to further probe their com-

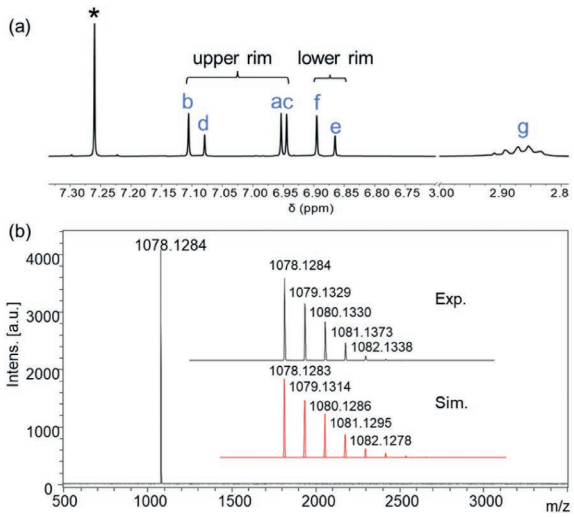


Fig. 2. Partial ^{1}H NMR (400 MHz, 298 K, $CDCl_3$) spectrum (a) and MALDI-TOF mass spectrometry (b) of **[7]CP**. * $CHCl_3$.

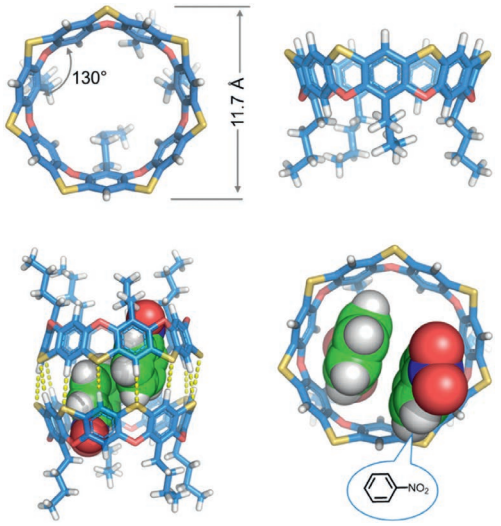


Fig. 3. X-rayed crystal structure of **[7]CP**. Color code: S = yellow, O = red, C = light blue or green, N = blue, H = white. C – H···S hydrogen bonds are highlighted in yellow lines.

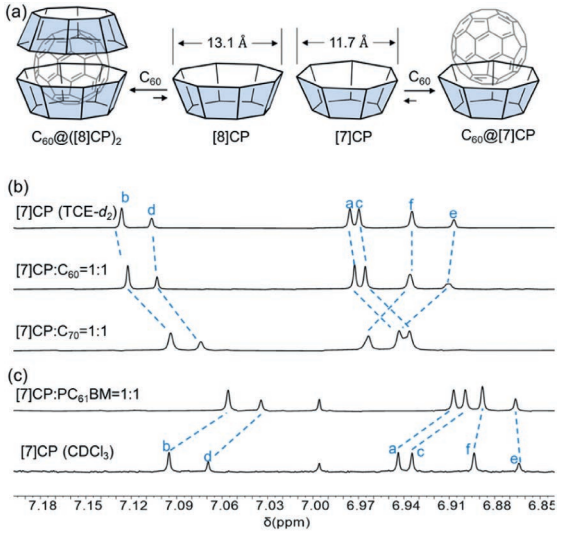


Fig. 4. (a) Schematic representation of complexation of C_{60} with **[8]CP** or **[7]CP**. (b, c) Partial ^{1}H NMR (400 MHz, 298 K) spectra of free **[7]CP** and its 1:1 mixture with C_{60}, C_{70}, and $PC_{61}BM$.

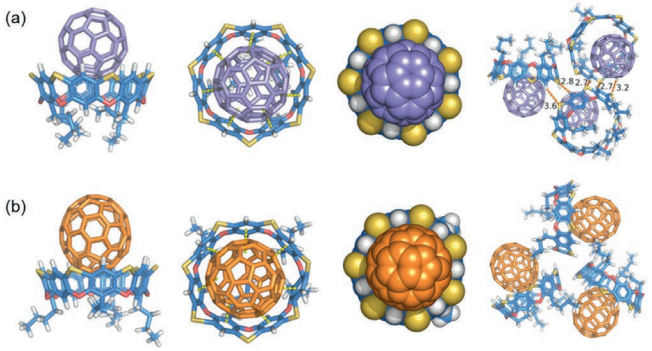


Fig. 5. X-rayed crystal structure of complex C_{60}**@[7]CP** (top) and **C_{70}@[7]CP** (bottom). Color code: S yellow, O red, C light blue, H white, C_{60} purple and C_{70} orange. $\pi-\pi$ interactions, and C–H···S hydrogen bonds are highlighted in yellow and orange lines, respectively.

plexation (Figs. 4b and c). The chemical shift of **[7]CP** changes upon complexing fullerenes (Table 1). All three complexes exhibit similar resonance shift trends, with the upper-rim protons H_a, H_b, H_c, and H_d shifting upfield, while the lower-rim protons H_e and H_f shift downfield. These results indicate a similar binding mode, with $\pi-\pi$ interactions likely occurring between the phenylene moieties and C_{60}, consistent with the behavior observed for the complexation of a methylated **[8]CP** with C_{60} [29]. A more pronounced chemical shift change was observed for the complexation of **[7]CP** with C_{70} compared to **[7]CP** with C_{60}, suggesting a stronger binding affinity for the C_{70}**@[7]CP** complex than for C_{60}**@[7]CP**. Indeed, fitting the ^{1}H NMR titration data in deuterated 1,1,2,2-tetrachloroethane afforded association constants (K_a) of 1638 and 2534 L/mol for C_{60}**@[7]CP** and C_{70}**@[7]CP**, respectively (Table 1 and Figs. S2 and S4 in Supporting information), confirming the inference from the NMR studies. The fullerene C_{60} derivative $PC_{61}BM$ retains the conjugated carbon sphere structure of C_{60} but features a larger substituent attached to its surface (Fig. 1). Therefore, it is expected to poess a similar binding behavior for the complexation of $PC_{61}BM$ by **[7]CP**. A K_a of 3682 L/mol was determined for the $PC_{61}BM$**@[7]CP** complex in deuterated chloroform (Fig. S6 in Supporting information). Thus, all these **[7]CP** complexes exhibit similar binding affinities, ranging from −4.3 to −4.8 kcal/mol, which are about two orders of magnitude lower than those of reported **[8]CP** complexes [28–31]. This can be attributed to the reduced cavity size of **[7]CP**, which prevents the formation of dimeric capsule-like complexes with fullerenes, as observed for **[8]CP**. Nevertheless, **[7]CP** has demonstrated its potential to function as a molecular container for fullerenes, exhibiting a 1:1 binding stoichiometry.

To further investigate the supramolecular chemistry of **[7]CP** with fullerenes, single crystals of the C_{60}**@[7]CP** and C_{70}**@[7]CP** complexes were successfully prepared and analyzed by X-ray crystallography (Table S1 in Supporting information). As shown in Fig. 5a, the crystal structure of C_{60}**@[7]CP** unambiguously confirms the formation of a 1:1 complex, consistent with the results obtained from UV–vis absorption and ^{1}H NMR analysis. Although **[7]CP** is predicted to be unable to fully accommodate a C_{60} molecule, partial insertion of the fullerene into the cavity of **[7]CP** occurs due to their retained convex–concave geometric complementarity, as evidenced by $\pi-\pi$ interactions with measured centroid-to-centroid distances of 3.8–4.1 Å. Multiple C–H···S hydrogen bonds (with CH···S distances of 2.7–3.6 Å) between adjacent nanobelts further stabilize the complex and extend the structure into a three-dimensional network. As revealed by ^{1}H NMR analysis, the crystal structure of the **[7]CP** and C_{70} complex confirms identical binding behavior, forming a 1:1 complex (Fig. 5b). C_{70} partially re-

Table 1
Chemical shift changes ($\Delta\delta$H) of **[7]CP** upon complexing with one equivalent of fullerene and binding constant (K_a) and free energy (ΔG) of the corresponding host-guest complexes.

Fullerene	$\Delta\delta$H (ppm)						K_a (L/mol) [a]	ΔG (kcal/mol)
	a	b	c	d	e	f		
C_{60}	−0.006	−0.008	−0.008	−0.007	+0.006	+0.002	1638	−4.3
C_{70}	−0.032	−0.032	−0.034	−0.033	+0.036	+0.029	2534	−4.5
$PC_{61}BM$	−0.037	−0.040	−0.035	−0.035	+0.002	−0.006	3682[b]	−4.8

[a] Determined by ^{1}H NMR titration at 298 K in deturated 1,1,2,2-tetrachloroethane.
[b] Measured in chloroform-*d*.

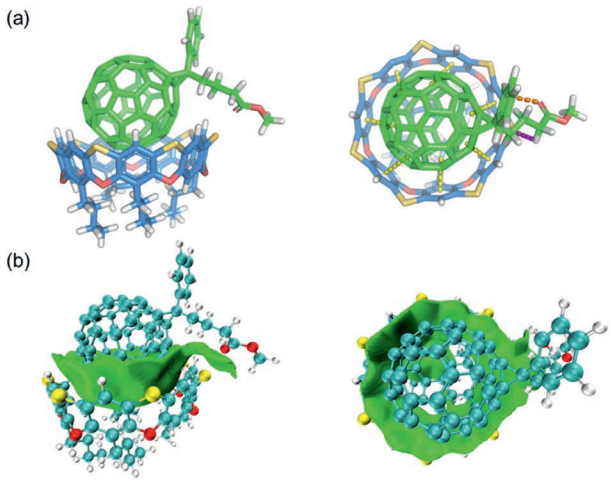


Fig. 6. DFT caculation optimized structure (a) and IGM (δginter = 0.001) analysis (b) of the complex $PC_{61}BM$**@[7]CP**. Color code: S yellow, O red, C light blue or green, H white. $\pi-\pi$ interactions, C−H···O and C−H···S hydrogen bonds are highlighted in yellow, orange and purple lines, respectively.

sides within the cavity of **[7]CP**, optimizing $\pi-\pi$ interactions, with centroid-to-centroid distances ranging from 3.7 Å to 4.3 Å. In contrast to the spherical C_{60}, C_{70} adopts an elongated, rugby ball shape, resulting in a more anisotropic electron density distribution. This curvature induces a slight polarization along its long axis, which leads to the shielding of the equatorial region and deshielding of the apical pentagons [34]. As a result, the larger chemical shift changes observed for **[7]CP** upon complexation with C_{70} can be attributed to the structure of their complex, where the upper-rim protons are located near C_{70}'s equatorial region, while the lower-rim protons are positioned closer to the deshielding apical pentagons. Such a complex structure likely contributes to the enhanced binding affinity of C_{70} compared to C_{60}.

Since attempts to obtain single crystals of the $PC_{61}BM$**@[7]CP** complex were unsuccessful, its structure was optimized using density functional theory (DFT) calculations (Fig. S7 in Supporting information) and compared with C_{60}**@[7]CP** and C_{70}**@[7]CP**. As shown in Fig. 6a, the calculated structure of $PC_{61}BM$**@[7]CP** exhibits a similar binding mode, with $PC_{61}BM$ partially inserted into the cavity of **[7]CP**. This interaction is primarily driven by convex−concave $\pi-\pi$ interactions, with optimized centroid-to-centroid distances ranging from 3.6 Å to 4.0 Å, as confirmed by independent gradient model (IGM) analysis (Fig. 6b) [35].

In conclusion, we successfully synthesized [7]cyclophenoxathiin (**[7]CP**), a nanobelt with a heptagonal frustum-shaped structure, using a multi-step approach. Host-guest interactions with fullerenes (C_{60}, C_{70}, and $PC_{61}BM$) revealed that **[7]CP** forms sTable 1:1 complexes. While the reduced cavity size prevents the formation of dimeric complexes seen with **[8]CP**, **[7]CP** still acts as an effective molecular container for fullerenes. This work enhances our understanding of smaller nanobelt host-guest chemistry and paves the way for multifunctional material design in organic electronics and nanotechnology. A comprehensive study of its host–guest chemistry towards small molecular guests and other physical properties is currently ongoing.

Declaration of competing interest

The authors declare that they have no known competing financial interests or personal relationships that could have appeared to influence the work reported in this paper.

CRediT authorship contribution statement

Zhenglin Du: Investigation. **Weijie Zhang:** Investigation. **Yisong Tang:** Investigation. **Xia Li:** Investigation. **Jialin Xie:** Writing – review & editing, Data curation, Investigation. **Kelong Zhu:** Validation, Project administration, Writing – review & editing, Supervision, Conceptualization.

Acknowledgments

We thank the National Natural Science Foundation of China (Nos. 22171295, 22471300, 22401064), the Fundamental Research Funds for the Central Universities (No. 23xkjc006), Science and Technology Projects in Guangzhou (No. 2024A04J6423), the Program for Guangdong Introducing Innovative and Entrepreneurial Teams (No. 2017ZT07C069) and Innovational Fund for Scientific and Technological Personnel of Hainan Province (No. KJRC2023D34) for financial support.

Supplementary materials

Supplementary material associated with this article can be found, in the online version, at doi:10.1016/j.cclet.2025.111499.

References

[1] K. Tahara, Y. Tobe, Chem. Rev. 106 (2006) 5274–5290.
[2] Z.F. Chen, D. Jiang, X. Lu, et al., Org. Lett. 9 (2007) 5449–5452.
[3] M.A. Majewski, M. Stępień, Angew. Chem. Int. Ed. 58 (2019) 86–116.
[4] K.Y. Cheung, S.J. Gui, C.F. Deng, et al., Chem 5 (2019) 838–847.
[5] K.Y. Cheung, Y. Segawa, K. Itami, Chem. Eur. J. 26 (2020) 14791–14801.
[6] E.S. Hirst, F. Wang, R. Jasti, Org. Lett. 13 (2011) 6220–6223.
[7] R. Gleiter, B. Esser, S.C. Kornmayer, Acc. Chem. Res. 42 (2009) 1108–1116.
[8] B. Esser, M. Hermann, Nat. Chem. 13 (2021) 209–211.
[9] E. Heilbronner, Helv. Chim. Acta 37 (1954) 921.
[10] P.R. Ashton, N.S. Isaacs, F.H. Kohnke, et al., Angew. Chem. Int. Ed. 27 (1988) 966–969.
[11] Y.M. Li, Y. Segawa, A. Yagi, J. Am. Chem. Soc. 142 (2020) 12850–12856.
[12] X.S. Du, D.W. Zhang, Y. Guo, et al., Angew. Chem. Int. Ed. 60 (2021) 13021–13028.
[13] T.H. Shi, S. Tong, M.X. Wang, Angew. Chem. 132 (2020) 7774–7779.
[14] T.H. Shi, M.X. Wang, CCS Chem. 3 (2021) 916–931.
[15] R. Zhang, D.Y. An, J.Y. Zhu, et al., Adv. Funct. Mater. 33 (2023) 2305249.
[16] T. Liu, L.X. Zhu, K. Liu, et al., J. Am. Chem. Soc. 146 (2024) 32445–32451.
[17] G. Povie, Y. Segawa, T. Nishihara, et al., Science 356 (2017) 172–175.
[18] M. Iyoda, J. Yamakawa, M.J. Rahman, Angew. Chem. Int. Ed. 50 (2011) 10522–10553.
[19] T.H. Shi, Q.H. Guo, S. Tong, et al., J. Am. Chem. Soc. 142 (2020) 4576–4580.
[20] Q. Zhang, Y.E. Zhang, S. Tong, et al., J. Am. Chem. Soc. 142 (2020) 1196–1199.

[21] H. Chen, Q. Miao, J. Phys. Org. Chem. 33 (2020) e4145.
[22] J.L. Wang, Q. Miao, Org. Lett. 21 (2019) 10120–10124.
[23] F. Zhang, X.S. Du, D.W. Zhang, et al., Angew. Chem. Int. Ed. 60 (2021) 15291–15295.
[24] J. Zhu, Y. Han, Y. Ni, et al., J. Am. Chem. Soc. 143 (2021) 2716–2721.
[25] S.H. Nishigaki, Y. Shibata, A. Nakajima, et al., J. Am. Chem. Soc. 141 (2019) 14955–14960.
[26] M.L. Tan, Q.H. Guo, X.Y. Wang, Angew. Chem. Int. Ed. 59 (2020) 23649–23658.
[27] J. Pfeuffer-Rooschüz, L. Schmid, A. Prescimone, et al., JACS Au 1 (2021) 1885–1891.
[28] J.L. Xie, X. Li, S.H. Wang, et al., Nat. Commun. 11 (2020) 3348.
[29] J.L. Xie, X. Li, Z.L. Du, et al., CCS Chem. 5 (2023) 958–970.
[30] Z.L. Du, J.L. Xie, Y.D. Liu, et al., Chem. Commun. 60 (2024) 6387.
[31] Y.D. Liu, S.H. Wang, J.L. Xie, et al., Chem. Asian J. 18 (2024) e202400626.
[32] S.C. Kornmayer, B. Esser, R. Gleiter, Org. Lett. 11 (2009) 725–728.
[33] S.H. Wang, J. Yuan, J.L. Xie, et al., Angew. Chem. Int. Ed. 60 (2021) 18443–18447.
[34] T. Iwamoto, Y. Watanabe, H. Takaya, et al., Chem. Eur. J. 19 (2013) 14061–14068.
[35] T. Lu, Q.X. Chen, J. Comput. Chem. 43 (2022) 539–555.